IMMUNODEFICIENCIES

Copyright © 2018 The Authors, some rights reserved; exclusive licensee American Association for the Advancement of Science. No claim to original U.S. Government Works

ZNF341 controls STAT3 expression and thereby immunocompetence

Stefanie Frey-Jakobs[1]*, Julia M. Hartberger[1]*, Manfred Fliegauf[1]*, Claudia Bossen[1]*, Magdalena L. Wehmeyer[1], Johanna C. Neubauer[1], Alla Bulashevska[1], Michele Proietti[1], Philipp Fröbel[1], Christina Nöltner[1], Linlin Yang[1], Jessica Rojas-Restrepo[1], Niko Langer[1], Sandra Winzer[1], Karin R. Engelhardt[2], Cristina Glocker[1†], Dietmar Pfeifer[3], Adi Klein[4], Alejandro A. Schäffer[5], Irina Lagovsky[6,7], Idit Lachover-Roth[8], Vivien Béziat[9,10], Anne Puel[9,10,11], Jean-Laurent Casanova[9,10,11,12,13], Bernhard Fleckenstein[14], Stephan Weidinger[15], Sara S. Kilic[16‡], Ben-Zion Garty[6,17‡], Amos Etzioni[18‡], Bodo Grimbacher[1,19,20‡§]

Signal transducer and activator of transcription 3 (STAT3) is a central regulator of immune homeostasis. STAT3 levels are strictly controlled, and STAT3 impairment contributes to several diseases including the monogenic autosomal-dominant hyper–immunoglobulin E (IgE) syndrome (AD-HIES). We investigated patients of four consanguineous families with an autosomal-recessive disorder resembling the phenotype of AD-HIES, with symptoms of immunodeficiency, recurrent infections, skeletal abnormalities, and elevated IgE. Patients presented with reduced STAT3 expression and diminished T helper 17 cell numbers, in absence of *STAT3* mutations. We identified two distinct homozygous nonsense mutations in *ZNF341*, which encodes a zinc finger transcription factor. Wild-type ZNF341 bound to and activated the *STAT3* promoter, whereas the mutant variants showed impaired transcriptional activation, partly due to nuclear translocation failure. In summary, nonsense mutations in *ZNF341* account for the STAT3-like phenotype in four autosomal-recessive kindreds. Thus, ZNF341 is a previously unrecognized regulator of immune homeostasis.

INTRODUCTION

Immune homeostasis in humans is important to avoid the two extremes of immunodeficiency and autoimmunity/autoinflammation. Signal transducer and activator of transcription 3 (STAT3) is an immune rheostat that prevents such diseases by regulating the innate and adaptive immune system (*1*). T helper 17 (T_H17) $CD4^+$ T cell differentiation and interleukin (IL)–17 production are dependent on precisely balanced STAT3 activity (*2*–*6*), and germline and somatic mutations in *STAT3* have been associated with multiple immune disorders and cancer, respectively (*7*). For instance, heterozygous germline gain-of-function (GOF) mutations lead to lymphoproliferation and juvenile-onset autoimmunity (*8*, *9*), whereas heterozygous loss-of-function (LOF) mutations in *STAT3* cause an autosomal-dominant (AD) immunodeficiency known as hyper–immunoglobulin E (IgE) syndrome [HIES; Online Mendelian Inheritance in Man (OMIM) #147060 and #243700] (*10*). STAT3-LOF mutations have been shown to exert a dominant-negative effect impairing antibacterial and antifungal host defense and resulting in a multisystem disorder also affecting the skeleton, dentition, and connective tissue (*11*, *12*). Patients present with the clinical triad of recurrent pneumonia, eczema with cold staphylococcal skin abscesses, and elevated serum IgE levels (*11*). *STAT3*-LOF mutations represent the underlying genetic defect in ~75% of sporadic and AD-HIES patients (OMIM: *102582), whereas biallelic *DOCK8* mutations account for disease in ~80% of patients with the autosomal-recessive (AR) form of HIES (OMIM: *611432) (*13*, *14*). In addition, mutations in *PGM3* (OMIM: *172100) (*15*, *16*) have been described in AR-HIES. At least one of these AR immunodeficiency syndromes also involves dysregulated STAT3 function because the lack of DOCK8 results in reduced STAT3 activation (*17*, *18*).

However, regulatory mechanisms of the STAT3 equilibrium are complex and not fully understood. Regulation at the protein level includes phosphorylations and interactions with other STAT family members (*19*). In addition, epigenetic regulation by HMGB1 (*20*) or ZNF382 (*21*) and transcriptional regulation of *STAT3* through STAT3 itself and other transcription factors have been proposed (*22*).

Here, we report that ZNF341, a previously uncharacterized C2H2 zinc finger transcription factor, is mutated in families with recurrent

[1]Center for Chronic Immunodeficiency, Medical Center University of Freiburg, Faculty of Medicine, University of Freiburg, Germany. [2]Primary Immunodeficiency Group, Institute of Cellular Medicine, Newcastle University, Newcastle upon Tyne, UK. [3]Department of Hematology, Oncology and Stem Cell Transplantation, Medical Center University of Freiburg, Faculty of Medicine, University of Freiburg, Germany. [4]Department of Pediatrics, Hillel Yaffe Medical Center, Faculty of Medicine, Technion-Israel Institute of Technology, Haifa, Israel. [5]National Center for Biotechnology Information, National Institutes of Health, Department of Health and Human Services, Bethesda, MD 20894, USA. [6]Sackler Faculty of Medicine, Tel Aviv University, Tel Aviv, Israel. [7]Felsenstein Medical Research Center, Rabin Medical Center, Petah Tikva, Israel. [8]Allergy and Immunology Clinic, Meir Medical Center, Kfar Saba, Israel. [9]Laboratory of Human Genetics of Infectious Diseases, Necker Branch, INSERM U1163, 75015 Paris, France. [10]Paris Descartes University, Imagine Institute, 75015 Paris, France. [11]St. Giles Laboratory of Human Genetics of Infectious Diseases, Rockefeller Branch, The Rockefeller University, New York, NY 10065, USA. [12]Pediatric Hematology–Immunology Unit, Necker Hospital for Sick Children, Assistance Publique des Hôpitaux de Paris, 75015 Paris, France. [13]Howard Hughes Medical Institute, New York, NY 10065, USA. [14]Institute of Clinical and Molecular Virology, University of Erlangen-Nürnberg, Erlangen, Germany. [15]Department of Dermatology, Venereology and Allergology, University Hospital Schleswig-Holstein, Campus Kiel, Kiel, Germany. [16]Department of Pediatric Immunology, Uludag University Medical Faculty, Gorukle-Bursa, Turkey. [17]Allergy and Immunology Clinic, Schneider Children's Medical Center, Tel Aviv, Israel. [18]Ruth's Children Hospital, Rambam Health Care Campus and Rappaport Faculty of Medicine, Technion-Israel Institute of Technology, Haifa, Israel. [19]Institute of Immunology and Transplantation, Royal Free Hospital and University College London, London, UK. [20]DZIF (German Center for Infection Research) Satellite Center Freiburg, Germany.
*These authors contributed equally to this work.
†Present address: Department of Cardiology and Pulmonology, Brandenburg Medical School, University Hospital Brandenburg, Brandenburg a. d. Havel, Germany.
‡These authors contributed equally to this work.
§Corresponding author. Email: bodo.grimbacher@uniklinik-freiburg.de

Downloaded from http://immunology.sciencemag.org/ by guest on September 27, 2020

bacterial and fungal infections. Two distinct homozygous nonsense mutations in exons 6 and 8 of *ZNF341* segregate with a phenotype resembling HIES in four consanguineous families with AR inheritance. We describe ZNF341 as a positive regulator of *STAT3* expression and report the clinical and laboratory phenotype of individuals lacking ZNF341.

RESULTS

STAT3-HIES–like phenotype with AR inheritance identified in four consanguineous families

We performed mutational analyses to identify the genetic defects in four consanguineous HIES families with AR inheritance in which mutations in known HIES genes had previously been excluded. The clinical triad of HIES consisting of recurrent pneumonias, eczema with cold skin abscesses, and elevated serum IgE levels was present in all three affected individuals (A.II.1, A.II.2, and A.II.3) of the consanguineous family A (for representative pictures of clinical findings, see Fig. 1; pedigree of family A in Fig. 2A). In addition, they showed skeletal/connective tissue abnormalities and formation of bronchiectasis and pneumatoceles (Fig. 1D) characteristic for STAT3-HIES and also suffered from recurrent candidiasis. Affected members of families B, C, and D (Fig. 2, B to D) presented with a milder phenotype initially diagnosed as atopic dermatitis, with characteristic HIES symptoms occurring later in life. The three Israeli families (families A, B, and C) are descendants from soldiers who lived in Sudan in the 19th century. Family D is of Turkish origin. Increased susceptibility to viral infections, typical in DOCK8-deficient AR-HIES, was not observed in any of the patients.

Reduced T_H17 $CD4^+$ T cell numbers in patients with STAT3-HIES–like phenotype

Immunophenotyping revealed normal CD19 lymphocyte counts, but an increased percentage of naïve B cells (IgD^+CD27^-) and reduced memory B cells ($CD27^+$) in the affected individuals. All memory B cell subpopulations including IgG^+, IgA^+, and IgM^+ were significantly reduced (fig. S1A). Patients had normal counts for naïve and memory $CD4^+$ and $CD8^+$ T cells, and for the $CD4^+$ subsets T_H1, T_H1* ($CCR6^+$ T_H1 cells), and T_H2 (fig. S1B). However, patients presented a significantly reduced percentage of T_H17 $CD4^+$ T cells, a key feature of STAT3-HIES (Fig. 2F, left). This coincided with reduced expression of CCR6, which is STAT3-dependent (*23*), in memory CD4 T helper cells (fig. S1B, lower right). In addition, peripheral blood mononuclear cells (PBMCs) derived from patients failed to differentiate into IL-17–producing $CD4^+$ T cells (Fig. 2F, right, and fig. S1C) and showed reduced numbers of IL-22^+ T cells (fig. S1D). Detailed case reports, clinical findings, and extended immune phenotyping can be found in the Supplementary Materials (sections S1 and S2, table S1, and fig. S1). Together, these findings support the hypothesis that patients with *ZNF341* mutations have a previously unrecognized AR immunodeficiency that clinically resembles AD-HIES due to mutations in *STAT3*.

Homozygous nonsense mutations in *ZNF341* causing the disease phenotype in four HIES families

Genetic defects in *STAT3* itself were excluded by sequencing of the exons, complementary DNA (cDNA), and the genomic promoter region (section S3). We therefore performed genetic linkage analysis of family A and subsequent whole-exome sequencing (WES) on two patients and one healthy sibling of family A (section S4). We identified a homozygous nonsense mutation in exon 6 of *ZNF341* (Chr20:32345116C>T; GRCh37; c.904C>T; p.Arg302*, R302* for isoform1; RefSeq NM_001282933.1), which was also present in all patients from families B and C (Fig. 2, A to C and E). At that time, the mutation was absent from the Single Nucleotide Polymorphism database, but it was later listed as rs746141726 with an allele frequency of 0.0017% and observed only in the heterozygous state. By targeted next-generation sequencing (NGS), we identified a second homozygous *ZNF341* nonsense mutation in exon 8 (Chr20:32349795C>T; GRCh37; c.1156C>T; p.Arg386*, R386* for isoform1) in family D, which segregated with the disease status (Fig. 2, D and E).

ZNF341 comprises 15 exons and encodes for three isoforms (RefSeq NM_001282933.1; NM_032819.4; NM_001282935.1; three additional noncoding variants are listed in Ensembl; table S2). Expression of mRNA was confirmed in several cell lines and PBMCs (section S5 and fig. S2). We focused on the longest isoform 1, an 854–amino acid protein with 12 C2H2 zinc finger domains but no other conserved domain (Fig. 2G) and with putative transcription factor activity (UniProt: Q9BYN7-1 and Gene Ontology annotation). Both identified mutations predict premature termination of translation, deleting 11 (p.Arg302*; 31.1 kDa) or 9 (p.Arg386*; 40.4 kDa) C2H2 zinc finger domains, respectively. As expected, full-length ZNF341 isoform 1 was absent in patient-derived (B.II.1, B.II.4, D.II.2, and D.II.4) Epstein-Barr virus (EBV)–transformed B cell lines (Fig. 3A, top).

Although the patients presented with high IgE levels, a review of the atopic dermatitis meta-analysis of the EArly Genetics and Lifecourse Epidemiology consortium of 10,788 atopic dermatitis cases and 30,047 controls (*24*) did not reveal any significantly associated variant after Bonferroni correction within locus 20q11.22 (ZNF341 ± 200 kb) (fig. S3). In addition, this locus was not reported in a published genome-wide association studies (GWAS) meta-analysis of allergic sensitization in 11,903 affected cases and 19,976 controls (*25*), and no associated variants within this locus are

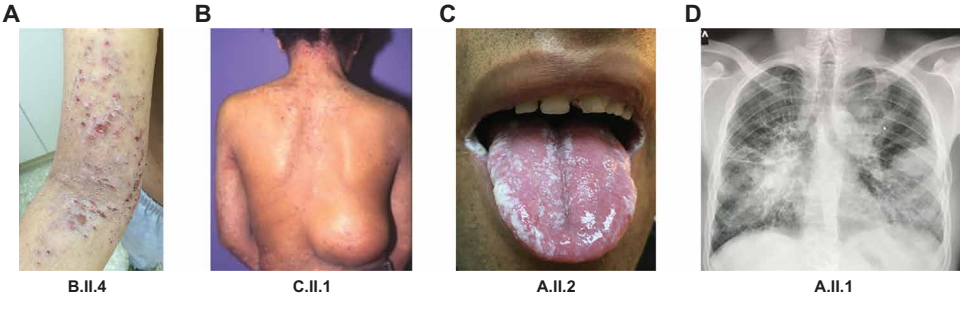

Fig. 1. Representative clinical and radiological manifestations in patients with homozygous *ZNF341* nonsense mutations. (**A**) Severe eczema in patient B.II.4 on the upper arm and cubital. (**B**) Patient C.II.1 with eczema on the neck and a cold skin abscess in the lumbar region missing the typical inflammatory signs of rubor, calor, and dolor. (**C**) Oral thrush due to *Candida* in patient A.II.2. (**D**) Chest radiograph of patient A.II.1 showing bilateral pneumonia with positive air bronchogram, bronchiectasis, and pneumatoceles.

Downloaded from http://immunology.sciencemag.org/ by guest on September 27, 2020

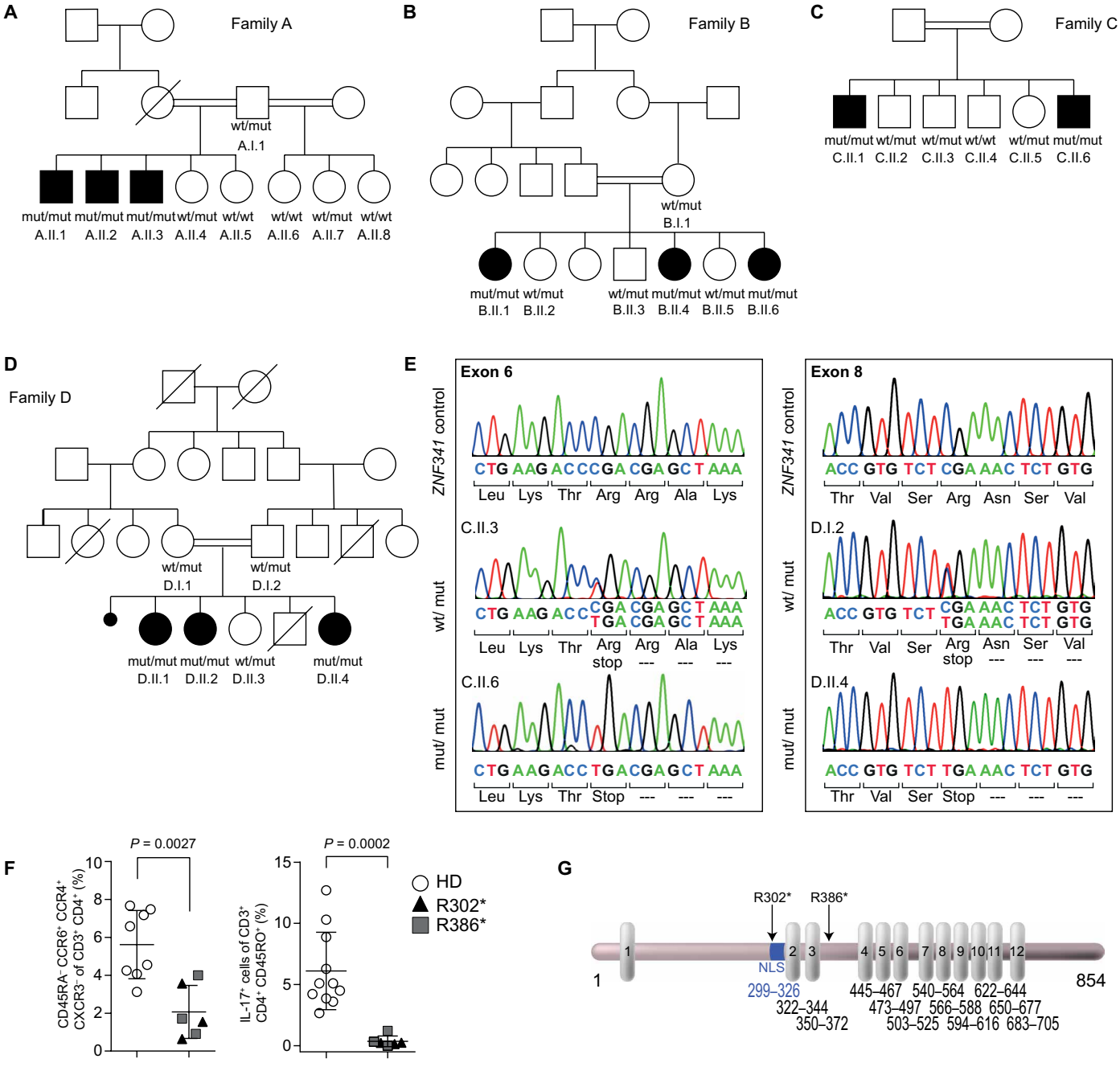

Fig. 2. Homozygous nonsense mutations in *ZNF341* cause HIES with reduced T_H17 cell numbers in patient PBMCs. (**A** to **D**) Pedigrees and genotypes with the nonsense mutated (mut) alleles g.32345116C>T (c.904C>T; p.Arg302*) for families A to C and g.32349795C>T (c.1156C>T; p.Arg386*) for family D. Heterozygous carriers are unaffected. Circles, female; squares, male; filled symbols, affected individuals with HIES; open symbols, healthy members; slash, deceased individual; double horizontal lines, consanguinity; black dot, miscarriage. (**E**) Both mutations predict premature termination of translation. (**F**) Flow cytometry of PBMCs demonstrate reduced T_H17 cell counts on the basis of $CD45RA^-CCR6^+CCR4^+CXCR3^-$ of $CD3^+CD4^+$ in patients ($n = 6$; triangles, family A; squares, family D) compared with HD controls (HD; $n = 8$; open circles) (left). In contrast to controls ($n = 11$), patient PBMCs ($n = 6$) fail to differentiate into IL-17^+ cells ($CD3^+CD4^+CD45RO^+$) upon in vitro stimulation (day 4) with T_H17-polarizing cytokines IL-1β and IL-6 plus T cell activation/expansion (right). Significance was determined using Mann-Whitney test. (**G**) ZNF341 is an 854–amino acid "zinc finger–only" transcription factor with 12 C2H2 motifs (vertical boxes). R302* and R386* (arrows) delete zinc fingers 2 to 12 and 4 to 12, respectively. A putative NLS (blue) is retained in the R386* mutant. Numbers indicate amino acid positions in NP_001269862.

listed in the current version of the National Human Genome Research Institute GWAS Catalog (www.ebi.ac.uk/gwas) (*26*) for atopy-related traits such as asthma, rhinitis, atopic dermatitis, and allergic sensitization.

Reduced *STAT3* mRNA and protein in patients with homozygous *ZNF341* nonsense mutations

To identify potential target genes of the ZNF341 transcription factor, we compared the transcriptomes of PBMCs derived from patient

Downloaded from http://immunology.sciencemag.org/ by guest on September 27, 2020

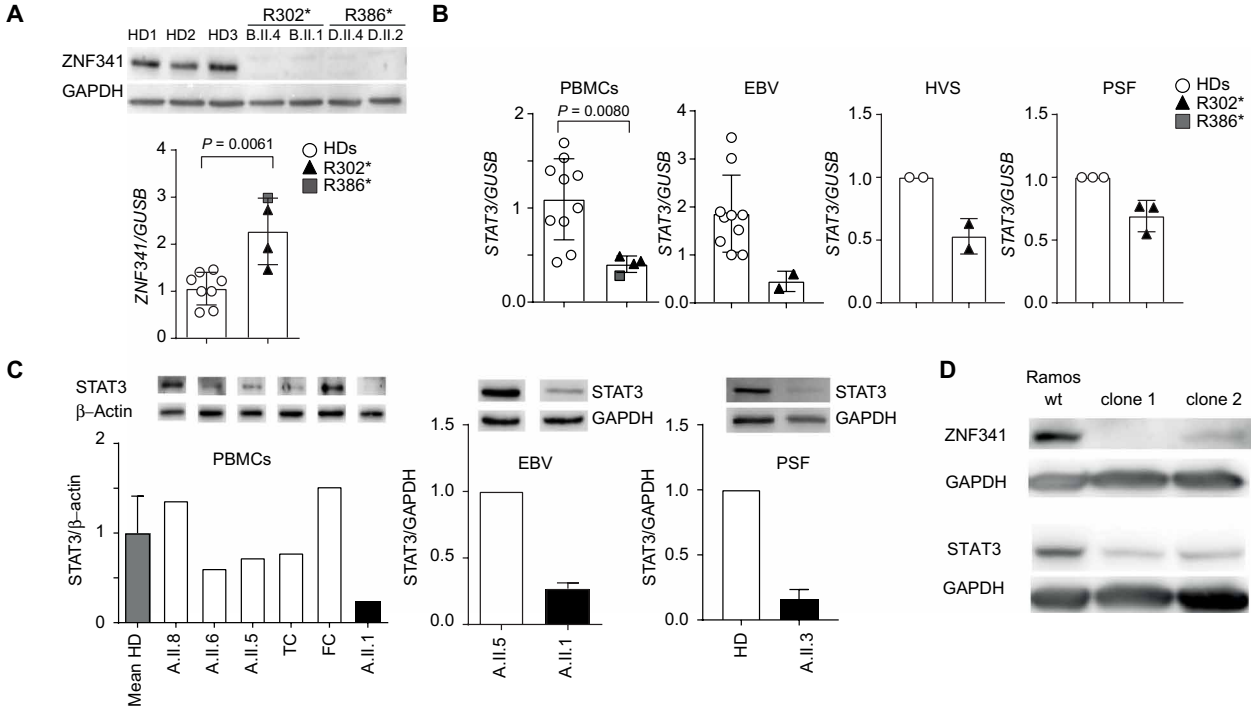

Fig. 3. Reduced STAT3 expression in patient-derived cells. (**A**) Full-length ZNF341 isoform 1 is undetectable in EBV cell lysates from patients with R302* (B.II.4 and B.II.1) and R386* (D.II.4 and D.II.2) mutations, respectively (top). Slightly increased relative *ZNF341* mRNA expression in patients' PBMCs (bottom; patients, $n = 4$; HD, $n = 8$). Data from independent experiments were normalized to mean of relative expression in controls. (**B**) Reduced *STAT3* mRNA expression in patient-derived cells. For PBMCs, data from independent experiments were normalized to mean of relative expression in controls (patients, $n = 4$; HD, $n = 10$). EBV cell lines: combined data from two independent experiments were normalized to relative expression of one control (patient A.II.1; HD, $n = 5$). HVS-transformed T cell line or PSFs of patient A.II.3 compared with HD [mean values and SD of two (HVS) or three (PSF) independent experiments]. (**C**) Western blot and quantitative densitometry demonstrate reduced STAT3 expression in patient-derived PBMCs, EBV cells, and PSF. β-Actin and GAPDH were used as loading controls. TC, travel control; FC, freezing control. (**D**) ZNF341 knockout in Ramos cells by using CRISPR/Cas9 technology showed reduced STAT3 protein expression in clones 1 and 2 in comparison to wt Ramos cells. GAPDH was used as loading control.

A.II.1 and his healthy sister A.II.5 (table S3) and confirmed the observations by real-time quantitative polymerase chain reaction (RT-qPCR) for additional individuals. *ZNF341* mRNA expression was variable and slightly increased in patients (A.II.1, A.II.2, A.II.3, and D.II.4), compared with healthy controls (Fig. 3A, bottom). However, *STAT3* mRNA expression was significantly reduced in PBMCs of all affected individuals (A.II.1, A.II.2, A.II.3, and D.II.4) compared with healthy controls (Fig. 3B, left).

These findings suggest that the STAT3-like HIES phenotype caused by *ZNF341* mutations could be associated with insufficient *STAT3* expression, presenting a previously unrecognized pathogenesis in addition to the well-described dominant-negative effect usually associated with *STAT3* mutations. Reduced *STAT3* mRNA expression was also observed in an EBV-transformed B cell line of patient A.II.1, in a Herpesvirus saimiri (HVS)–transformed T cell line of patient A.II.3, and in primary skin fibroblasts (PSFs) of patient A.II.3 (Fig. 3B). Moreover, STAT3 protein expression was reduced in *ZNF341*-mutant cells (patients' PBMCs, EBV-transformed B cells, and PSFs), down to 15.5 to 27% of wild-type (wt) levels (Fig. 3C). Along the same lines, knockout of *ZNF341* in Ramos B cells by clustered regularly interspaced short palindromic repeats (CRISPR)/Cas9 technology showed reduced STAT3 protein expression (Fig. 3D). Furthermore, STAT3 Y705 phosphorylation was markedly impaired in PBMCs from patients with R302* and R386* mutations, respectively, after stimulation with IL-6 (Fig. 4A) or with interferon-α (IFN-α) in EBV cells from patient A.II.1 (Fig. 4B, left). Impaired STAT3 Y705 phosphorylation upon stimulation was even more obvious in EBV cell lines from two patients (B.II.1 and B.II.4) (Fig. 4B, right), indicating that reduced total STAT3 levels consequently lead to overall reduced phospho-STAT3 levels. Given we had excluded genetic defects in *STAT3* itself, we conclude that the mutations in *ZNF341* account for the HIES-phenotype because of the incapability of mutant cells to increase STAT3 protein expression and STAT3 phosphorylation above basal levels, leading to an imbalanced STAT3/phospho-STAT3 ratio in affected individuals.

Binding of ZNF341 to the *STAT3* promoter and subsequent activation of transcription

We next confirmed the transcriptional activation of the endogenous *STAT3* promoter upon transient overexpression of green fluorescent protein (GFP)–fused ZNF341 in human embryonic kidney (HEK) 293T cells (fig. S4). In contrast to the R302* mutant, wt ZNF341 caused a twofold increase of *STAT3* mRNA expression (fig. S4A). Using fluorescence-based reporter assays with synthetic promoters, composed of a genomic *STAT3* fragment (−535/−33 relative to the transcription start) fused to the cytomegalovirus (CMV) minimal promoter, we observed an average 2.9-fold increase of reporter expression over basal activity upon cotransfection with wt ZNF341, whereas only marginal activation (average 1.4-fold) was observed with the R302* mutant ZNF341 after 48 hours (Fig. 5, A and B). Increased reporter activity (average 2.6-fold) was also observed with the overexpressed ZNF341 variant R386* [which yielded much higher

Downloaded from http://immunology.sciencemag.org/ by guest on September 27, 2020

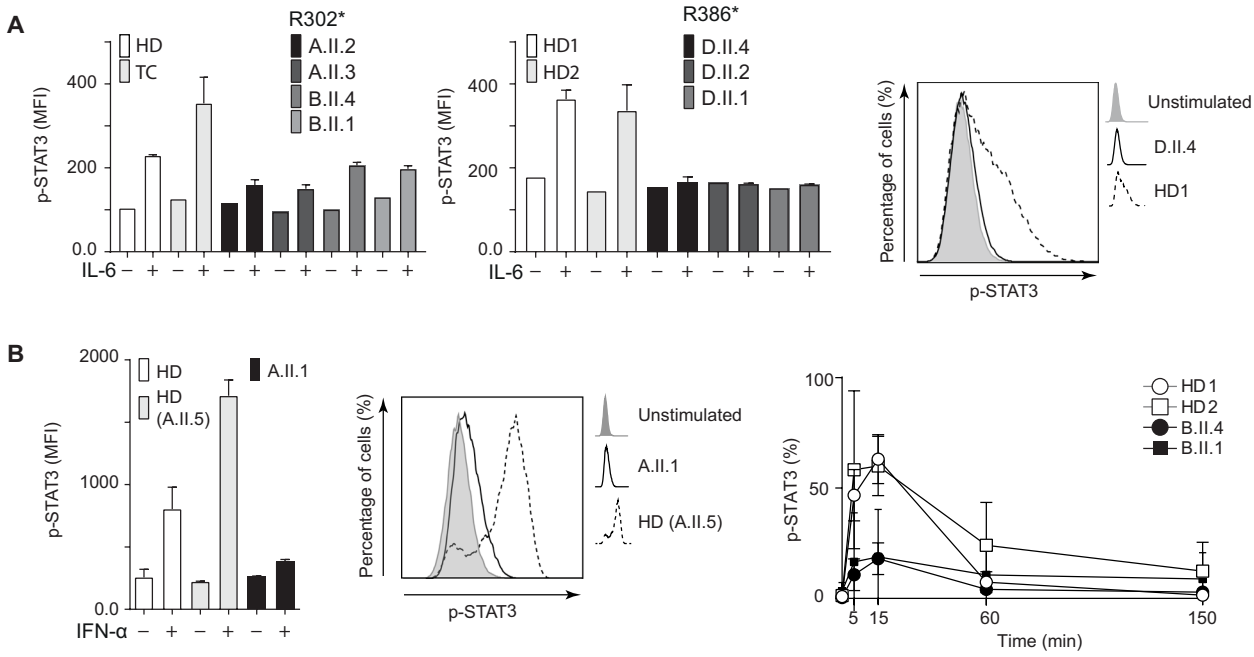

Fig. 4. Patients' primary T cells and EBV-transformed B cell lines showed reduced Y705 phosphorylation of STAT3. (**A**) Impaired IL-6 induced Y705 phosphorylation of STAT3 in patients' PBMCs (gate $CD3^+$) compared with healthy controls. (**B**) Reduced phospho-STAT3 (p-STAT3) in IFN-α–treated EBV cells from patients with R302* mutations (left). Bar graphs show SD of duplicates; MFI, mean fluorescence intensity. Representative histograms (middle) demonstrating reduced p-STAT3 in patient (solid line) compared with control (dashed line). Shaded area, unstimulated cells. Only marginal transient increase of p-STAT3 in patients 15 min after stimulation (right). Baseline p-STAT3 levels are reached within 150 min after stimulation. Mean values from independent experiments (HD1, HD2, and B.II.4, $n \geq 3$; B.II.1, $n = 2$) are shown.

expression levels than the wt protein (fig. S4C)], suggesting that residual transcription factor activity is retained (Fig. 5, A and B). Similar results were obtained with longer (−997/−33) and shorter (−476/−33) *STAT3* promoter fragments and at variable time points (fig. S5).

To determine whether ZNF341 directly regulates *STAT3* by binding to its promoter, we searched for ZNF341 binding sites by chromatin immunoprecipitation sequencing (ChIP-seq). ChIP-seq data, obtained with two different antibodies recognizing ZNF341, were highly correlated (fig. S6A). We identified 1658 high-confidence ZNF341 binding sites genome-wide, with a high proportion being located at promoters or within short distance to promoters (<1 kb) (Fig. 5C). The *STAT3* promoter displayed high ZNF341 occupancy (Fig. 5D), which was confirmed by ChIP (fig. S6B). This was not observed in patient-derived cells, highlighting the specificity of the antibody as well (fig. S6C). Thirty-six binding sites, termed super-binding sites, were characterized by high level of ZNF341 occupancy (Fig. 5E) and accounted for about half of ZNF341 occupancy (as determined by normalized tag count) (Fig. 5F). Expression of the genes associated with the top two binding sites (*STAT3* and *KAT6A*) was decreased in patient-derived PBMCs compared with a healthy control, further supporting the role of ZNF341 as a transcriptional activator (table S3). To identify the sequence recognized by ZNF341, we performed de novo motif analysis. A 10-nucleotide (nt) motif was highly enriched at ZNF341 binding sites, as well as a separate 10-nt G-rich motif (Fig. 5G). When searching for longer motifs, we identified a 30-nt sequence, which contained both 10-nt motifs (Fig. 5H, top), located at position −217/−187 in the *STAT3* promoter region (relative to the transcription start). This motif could be further refined in the super-binding sites (Fig. 5H, bottom), suggesting that ZNF341 uses several zinc fingers for DNA binding, whereas the remaining zinc fingers may contribute to preferential binding. This might explain why half of ZNF341 occupancy occurs at only 36 preferential binding sites. Thus, ZNF341 has the potential to recognize a highly specific sequence and therefore to regulate a limited number of genes, including *STAT3*.

Aberrant cytoplasmic localization of nuclear ZNF341 caused by the R302* mutation

We further characterized the molecular defects of the *ZNF341* nonsense mutations by transient overexpression in HEK293T cells (fig. S4). The wt ZNF341 achieved moderate protein levels [regardless of whether it is fused to enhanced GFP (EGFP)], whereas both truncated proteins (R302* and R386*) were expressed at higher levels (fig. S4, B and C; for expression levels, see also figs. S5B and S7, C and D). Confocal microscopy (Fig. 5I) of EGFP-fused constructs showed that the wt ZNF341 localized to the nucleus, as predicted by the protein atlas. In contrast, truncated EGFP-ZNF341-R302* remained in the cytoplasm, indicating that the nuclear localization sequence (NLS) was deleted. Thus, the inability of the R302* mutant to contribute to transcriptional activation is most likely due to the failure of nuclear translocation, and, accordingly, we did not detect any binding of ZNF341 variant R302* to chromatin (figs. S6C and S7, A and B). Unexpectedly, the truncated mutant EGFP-ZNF341-R386* retained its ability to localize to the nucleus (Fig. 5I). Thus, a potential NLS, which is predicted to reside between K299 and Y326 (http://nls-mapper.iab.keio.ac.jp/cgi-bin/NLS_Mapper_form.cgi), is sufficient for nuclear translocation of ZNF341-R386*. Nevertheless, the ZNF341-R386* variant showed reduced binding

Downloaded from http://immunology.sciencemag.org/ by guest on September 27, 2020

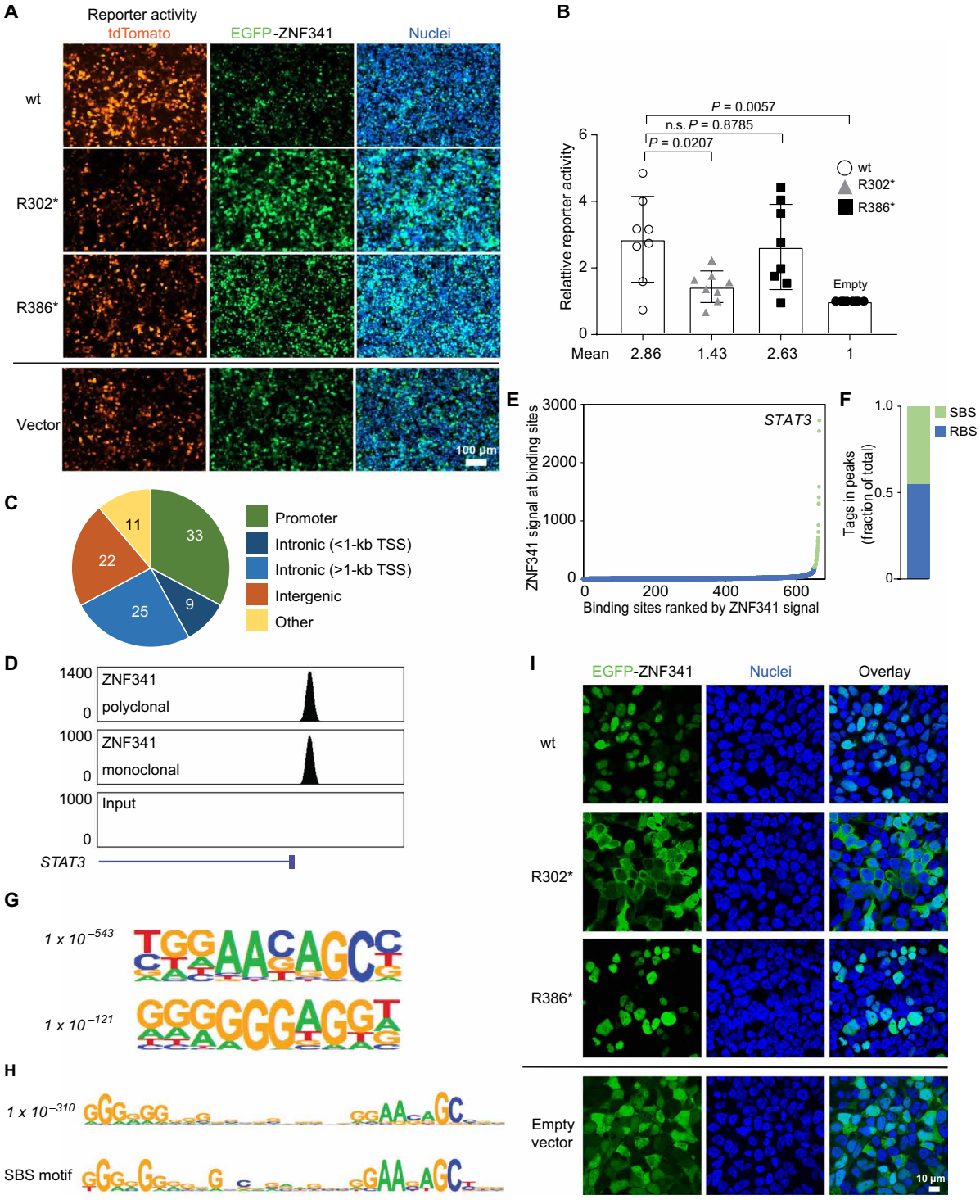

Fig. 5. ZNF341 binds to the *STAT3* promoter. (**A**) Activation of a synthetic *STAT3* promoter (with the −535/−33 upstream genomic sequence fused to the CMV minimal promoter) driving a red fluorescence (tdTomato) reporter upon cotransfection with EGFP-tagged wt or mutant ZNF341 in HEK293T cells (48 hours). Scale bar, 100 µm. (**B**) Relative reporter activity in two independent experiments in quadruplicate. Significance and *P* values were determined with Mann-Whitney test. n.s., not significant. (**C**) ChIP-seq analysis of ZNF341, performed with distinct antibodies, on EBV-transformed B cells reveals 1658 ZNF341 binding sites across various genomic regions and (**D**) shows high tag densities on the *STAT3* promoter region (Chr17: 40,530,000 to 40,545,000, hg19 build; normalized tags). (**E**) Distribution of ZNF341 ChIP-seq signal across the 1658 binding sites. Green, 36 super-binding sites (SBS) with >200 normalized tags; blue, remaining binding sites (RBS). (**F**) Normalized tags in SBS and RBS as a fraction of total. (**G**) Cis-regulatory sequences associated with ZNF341 occupancy. *P* values (italics) reflect the significance of motif occurrence. (**H**) A 30-nt cis-regulatory sequence associated with ZNF341 occupancy (*P* value as above) and with ZNF341 occupancy in SBS. (**I**) Representative confocal images of transfected HEK293T (48 hours) showing nuclear localization of EGFP-tagged wt ZNF341 and R386*, whereas R302* remains cytoplasmic. Scale bar, 10 µm.

Downloaded from http://immunology.sciencemag.org/ by guest on September 27, 2020

to chromatin in an overexpression system (fig. S7, A and B). Because ZNF341-R386* lacks 9 of the 12 zinc finger domains, residual transcription factor activity may occur only upon massive overexpression in vitro. However, the clinical phenotype suggests that the three remaining zinc fingers are insufficient for ZNF341-R386* binding to and activation of target promoters at physiological levels.

DISCUSSION

Janus kinase (JAK)–STAT signaling pathways have emerged as critical rheostats for the maintenance of cellular homeostasis, relevant to many human diseases (*27*–*29*). Impaired JAK-STAT signaling causes either immunodeficiency if decreased (*30*–*32*) or lymphoproliferative disorders if increased (*8*, *9*, *33*). Hence, the regulation of the amount of STAT (and JAK) signaling molecules and their phosphorylation status seem to determine the outcome of cellular signaling events. For example, LOF mutations in *STAT1* lead to susceptibility to viral and mycobacterial infections (*34*, *35*), whereas GOF mutations in the very same gene lead to a polarization of T lymphocytes away from the T_H17 $CD4^+$ T cell lineage toward the T_H1 lineage, leading to an increased susceptibility to recurrent fungal infections (*36*–*38*).

Furthermore, decreased STAT3 signaling due to dominant-negative mutations (*10*, *12*) leads to immunodeficiency characterized by the loss of T_H17 $CD4^+$ T cells (*3*–*5*). In contrast, somatic GOF mutations in *STAT3* lead to large granular lymphocytosis (*39*), and germline GOF mutations in *STAT3* lead to a complex immune-dysregulation syndrome (*8*, *9*). Therefore, the mechanisms controlling these cellular regulators (i.e., the transcription factors of the JAK and STAT molecules) become of central importance in human disease. JAK and STAT inhibitors have already been used to treat lymphoma/cancer, autoimmune diseases such as rheumatoid arthritis (*40*), and impaired infection control (*41*, *42*).

Here, we describe a transcription factor, ZNF341, regulating transcription of *STAT3*. As in HIES patients with *STAT3*-LOF mutations, the impairment of ZNF341 signaling also led to defective differentiation of naïve T cells into T_H17 cells (and hence IL-17 production), a process critically dependent on STAT3. Thus, we found that ZNF341 transcriptionally regulates *STAT3* expression, at least its increase above a certain basal level of transcription, but other aspects of the underlying mechanism of impaired JAK-STAT signaling due to homozygous nonsense mutations in *ZNF341* still need to be elucidated. Although reduction of ZNF341 reduces expression of STAT3, there may be more complex regulatory mechanisms involved, which await further elucidation. Likewise, whether the phenotype results mainly/exclusively from disrupted STAT3 levels or also from the dysregulation of other genes by mutant ZNF341 remains unclear. Although the mutated proteins can be expressed in an overexpression system, in patient cells mutated proteins escaped our detection by the available antibodies. However, with the development of more specific N-terminal antibodies, the question of retained translation of a mutated shortened ZNF341 in patients will be solved. This will be important to clarify whether the R386* mutation disturbs transcriptional activity of ZNF341 by inexpressibility or nonsense-mediated decay of the truncated protein or by other mechanisms affecting nuclear transcription. Moreover, homodimerization or heterodimerization of ZNF341 was not investigated.

Although our patients presented with high IgE levels, to date, *ZNF341* has not been associated with atopy-related traits such as asthma, rhinitis, atopic dermatitis, and allergic sensitization (*24*–*26*). Because ZNF341 comprises 12 zinc fingers, and because one zinc finger shows preference to a specific nucleotide triplet (*43*), ZNF341 has the potential to recognize a very specific sequence and regulate a limited number of genes, which is supported by the super-binding sites and motif analysis. In this regard, *KAT6A*, the gene whose promoter has the second top binding site by ChIP, was down-regulated in the transcriptome analysis (table S3). Mutations in *KAT6A* were recently identified in patients presenting with neurodevelopmental disorders (*44*). Lower *KAT6A* expression may contribute to the intellectual disabilities observed in our patients. Our data show that ZNF341 acts as a transcriptional activator for cytokine-mediated *STAT3* expression. Zinc finger transcription factors lacking other functional domains have been described to recruit either transcriptional activators or repressors or both (*45*). Overexpressed ZNF341 has been described to bind to PAF1, which plays a role in transcriptional elongation (*45*), supporting a role for ZNF341 as a transcriptional activator.

In summary, the transcription factor ZNF341 is a positive regulator of *STAT3* expression. Homozygous nonsense mutations in *ZNF341* lead to insufficient STAT3 levels, which prevent T_H17 cell differentiation and cause HIES-like phenotypes with recurrent infections. Thus, the well-known HIES phenotype not only is associated with well-described dominant-negative *STAT3* mutations but also can result from insufficient levels of otherwise normal STAT3.

Our observations also have pivotal importance regarding future intervention strategies in STAT3-dependent HIES. Because HIES can be caused by STAT3 insufficiency, gene therapeutic attempts aiming at the inactivation of the mutant allele to eliminate dominant-negative *STAT3* mutations should be carefully considered. On the other hand, treating STAT3-insufficient cells with recombinant ZNF341 might improve infection control. An interesting aspect in future research will be the link between ZNF341 and the maintenance of normal IgE levels, particularly in the context of allergy. Our patients with ZNF341 deficiency had highly elevated serum IgE levels. Hence, augmentation of ZNF341 function may normalize IgE production, possibly by interfering with T_H2 cell subset differentiation.

MATERIALS AND METHODS

Study design

The aim of this study was to characterize the underlying genetic defect and pathomechanism in a consanguineous AR-HIES family without mutations in known HIES genes. After the identification of *ZNF341* (encoding a transcription factor regulating *STAT3*) as the disease-causing gene in family A, additional families with unexplained AR-HIES were tested for *ZNF341* mutations.

Patients and controls

The study was conducted under protocols for human subjects. Samples were collected with the written consent of all study participants and/or their parental guardians after formal ethical approval by the local ethics committees at the University of Freiburg (ethics protocol numbers 239/99_120733 and 302/13), the Rambam Medical Center, the Children's Medical Center of Israel, Uludag University Medical Faculty, and collaborating institutions. Healthy family members were sequenced for the *ZNF341* mutation, and wt/wt family members were included into the healthy donor (HD) control group.

Downloaded from http://immunology.sciencemag.org/ by guest on September 27, 2020

Sample preparation

Human PBMCs were isolated by Ficoll density gradient centrifugation and either immediately used or frozen and stored in liquid nitrogen. EBV-transformed lymphoblastic B cell lines and HVS-immortalized T cell lines were generated from PBMCs by standard methods. PSFs were generated from a skin biopsy of patient A.II.3 by standard methods, and HD PSFs were provided by the lab of G. Finkenzeller.

Flow cytometry

Immunophenotyping of PBMCs was performed by staining for various cell surface markers. A list of the fluorochrome-conjugated antibodies and the applied gating strategy can be found in section S6.

STAT3 phosphorylation

For analysis of STAT3 expression and STAT3 phosphorylation, PBMCs were used either unstimulated or stimulated with human recombinant IL-6 (0.5 μg/ml; PeproTech, Hamburg, Germany) for 15 min at 37°C. EBV-transformed B cell lines were stimulated with IFN-α (0.5 μg/ml; PeproTech, Hamburg, Germany) for 5, 15, 60, and 150 min at 37°C. Cells were fixed (Lyse/Fix buffer, BD Biosciences) and permeabilized (Fix/Perm III buffer, BD Biosciences) according to the manufacturer's instructions. Cells were stained with anti–STAT3-FITC (fluorescein isothiocyanate; clone #232209; R&D Systems, Wiesbaden-Nordenstadt, Germany), anti-CD19 BV421 (clone HIB19, BioLegend), phospho-specific PE-coupled anti-STAT3 (pY705) antibodies (clone 4/P-STAT3, BD Biosciences), or CD3-FITC (clone SK7, BD Biosciences). Fixable viability dye eFluor 506 (eBioscience, Frankfurt, Germany) was used according to the manufacturer's instructions.

In vitro T_H17 cell differentiation

For in vitro differentiation assays, freshly purified PBMCs were stimulated with anti-CD2–, anti-CD3–, and anti-CD28–coated beads using a T cell activation/expansion kit according to the manufacturer's instructions (Miltenyi Biotec, Bergisch Gladbach, Germany), in combination with IL-1β (10 ng/ml) and IL-6 (50 ng/ml) or transforming growth factor–β (5 ng/ml) and IL-21 (25 ng/ml) for 4 days. Before and after induction, cells were stimulated for 4 hours with phorbol 12-myristate 13-acetate (50 ng/ml) and ionomycin (1 μg/ml) (both from Sigma-Aldrich) in the presence of brefeldin A (5 μg/ml; BD Biosciences). Cells were stained for surface markers with anti-CD4 PercP-Cy5.5 (clone RPTA-T4, BD Biosciences), anti-CD45RO PE-Cy7 (clone UCHL1, eBioscience), and anti-CD3 APC H7 (clone SK7, BD Biosciences); fixed; and permeabilized using a Cytofix kit (BD Biosciences). For intracellular staining, anti–IFN-γ FITC (clone B27, BD Biosciences) and anti–IL-17 PE (clone eBio64DEC17, eBioscience) were used. Fixable viability dye eFluor 506 (eBioscience, Frankfurt, Germany) was used according to the manufacturer's instructions.

All flow cytometry data were acquired on a FACSCanto II flow cytometer (BD Biosciences) and analyzed using FlowJo version X analysis software (Treestar, Ashland, OR).

RNA isolation, cDNA generation, qPCR, and cDNA sequencing

Total RNA, from PBMCs, EBV cell lines, HVS-transformed T cell lines, PSFs, HEK293T cells, or further cell lines, was isolated with the RNeasy Mini Kit using QIAshredder and column DNA digestion (Qiagen). cDNA was synthesized with QuantiTect reverse transcription kit (Qiagen). qPCR was performed in duplicate or triplicate using SYBR Green reagents (Qiagen or Thermo Fisher Scientific) and primers for *STAT3*, *ZNF341*, and the housekeeping gene *GUSB*. Fluorescence intensities were monitored over 40 cycles on a StepOne real-time PCR system (Applied Biosystems/Thermo Fisher Scientific) and relative mRNA expression was calculated with the $2^{-\Delta\Delta Ct}$ method. The *STAT3* cDNA sequences were analyzed using long-range PCRs with Q5 High-Fidelity DNA Polymerase (New England BioLabs) and Sanger sequencing. The most important primer sequences can be found in the Supplementary Materials, and all primer sequences are available upon request.

Western blotting

Fresh or frozen PBMCs, EBV-transformed B cells, PSFs, or transfected HEK293T lysates were used for blotting. Membranes were probed with primary antibodies separately for STAT3 (MAB1799; R&D Systems), ZNF341 [Atlas Antibody HPA024607 (polyclonal) or customized antibody (monoclonal)], glyceraldehyde-3-phosphate dehydrogenase (GAPDH) (G9295; Sigma-Aldrich), or β-actin (NB 600-532; Novus Biologicals). A detailed protocol can be found in section S6.

CRISPR/Cas9-mediated genome editing

ZNF341 knockout cells were generated using CRISPR/Cas9 technology. A guide RNA (gRNA) with high target specificity was selected using the CRISPR design tool from the Massachusetts Institute of Technology (http://crispr.mit.edu). The gRNA (CGTCGGGTCTTCAGCGTTGC) was targeting a region close to R302 and was cloned in the pX330-U6-Chimeric_BB-CBh-hSpCas9 plasmid, a gift from F. Zhang (Addgene plasmid #42230). $ZNF341^{-/-}$ clones were generated by single-cell sorting of EGFP-positive Ramos cells cotransfected with pX330-ZNF341-gRNA and an EGFP plasmid (1:10 ratio) in 96-well plates. After about 3 weeks, clones were screened by Western blot analysis.

Expression vectors and fluorescence-based promoter-reporter assay

The cDNAs for isoform 1 of wt ZNF341 and mutant ZNF341-R302* were cloned from patient-derived samples by reverse transcription (RT)–PCR. Mutant ZNF341-R386* was generated by site-directed mutagenesis. For transient transfection in HEK293T cells, expression vectors for EGFP-fused or nonfused versions were used (pEGFP-C1 and pEGFP-N1; Takara/Clontech) with the empty vectors as controls. Cells were transfected with X-tremeGENE HP reagent (Roche) and harvested 48 hours after transfection for RNA or protein analyses.

For the fluorescence-based promoter-reporter assay, three genomic fragments of the human *STAT3* promoter, comprising the upstream sequence from −997 to −33, from −535 to −33, or from −476 to −33 relative to the putative transcription start site (*46*), were amplified by PCR and fused to a 58–base pair (bp) CMV minimal promoter (without specific transcription factor binding sites). The synthetic promoter constructs provide a TATA box and an artificial transcription start site and drive the expression of a red fluorescent tdTomato reporter protein (Takara/Clontech). Expression vectors for nonfused or EGFP-fused wt ZNF341, mutant ZNF341-R302*, or mutant ZNF341-R386*, respectively, were cotransfected with the reporter into HEK293T cells using X-tremeGENE HP (Roche) transfection reagent. The empty vector pEGFP-C1 (without *ZNF341* cDNA) was used as control. Reporter assays ($n = 4$) were performed in 48-well plates in quadruplicate and evaluated with a Fluorospot reader at variable time points (48/72/96 hours; repeated measurements per plate at two distinct time points each). Reporter constructs containing

Downloaded from http://immunology.sciencemag.org/ by guest on September 27, 2020

only the CMV minimal promoter (without *STAT3* upstream sequences) and retinoic acid receptor-related orphan receptor C (*RORC*) and *IL-17A* promoter constructs (both fused to CMVmin) were confirmed to be nonactivatable by ZNF341 in independent experiments. Cells were analyzed for green (expression and subcellular localization of GFP-fused ZNF341) and red fluorescence (reporter activity) by conventional epifluorescence microscopy on a Zeiss Axiovert 200. Images were processed using the Zen software (Zeiss). Fluorescence intensities were measured on a Fluorospot analyzer (CTL, Bonn, Germany) and quantified using ImageJ software.

ChIP and ChIP-seq

Cells were fixed for 15 min in 1% formaldehyde in phosphate-buffered saline (PBS) with 2% fetal calf serum. Formaldehyde was quenched for 10 min with 0.2 M glycine. Cells were washed two times with ice-cold PBS. Protein G Dynabeads (30 μl; Life Technologies) were blocked with 0.5% bovine serum albumin (w/v) in PBS. Magnetic beads were bound with 5 μg of anti-ZNF341 antibody [Atlas Antibodies HPA024607 (polyclonal) or customized antibody (monoclonal)] or control rabbit IgG (Santa Cruz Biotechnology, sc2027x). Cross-linked cells were lysed in lysis buffer (0.5% NP-40, 10 mM Hepes, 85 mM KCl, and 4 μl of EDTA). After centrifugation, nuclei were resuspended and sonicated in sonication buffer [50 mM tris-HCl (pH 8.0), 1% SDS, and 10 mM EDTA] for five cycles at 10 s each on ice (20 W) with 50 s on ice between cycles. Lysates were cleared by centrifugation, and Triton X-100 was added at a final concentration of 1%. Lysates were then incubated overnight at 4°C with the previously prepared magnetic beads. Beads were washed once with radioimmunoprecipitation assay (RIPA) buffer [50 mM tris-HCl (pH 8.0), 150 mM NaCl, 0.1% SDS, 0.1% Na-deoxycholate, 1% Triton X-100, and 1 mM EDTA], once with RIPA 500 buffer [50 mM tris-HCl (pH 8.0), 500 mM NaCl, 0.1% SDS, 0.1% Na-deoxycholate, 1% Triton X-100, and 1 mM EDTA], once with LiCl wash [10 mM tris-HCl (pH 8.0), 250 mM LiCl, 0.5% NP-40, 0.5% Na-deoxycholate, and 1 mM EDTA], and lastly twice with TE buffer [10 mM Tris (pH 8.0) and 1 mM EDTA]. Bound complexes were eluted from the beads in elution buffer [10 mM tris-HCl (pH 8.0), 0.5% SDS, 300 mM NaCl, and 5 mM EDTA] for 30 min at 65°C with shaking. Cross-links were reversed overnight at 65°C. RNA and protein were digested in the supernatant using ribonuclease A and proteinase K. DNA was purified using ChIP DNA clean and concentrator columns (Zymo Research). ChIP primers are listed in section S6. ChIP results are represented as percent of input by dividing the signals obtained by the ChIP by the signals obtained from the input sample. For ChIP-seq, libraries were prepared with the NEBNext primer set and were size-selected with AMPure XP beads (Beckman Coulter). Libraries were run on Illumina HiSeq 2000. Reads were aligned to hg19 using Bowtie with the parameter –m 1 (http://bowtie-bio.sourceforge.net). Data were analyzed using HOMER (http://homer.salk.edu/homer). To correlate ChIP-seq data obtained with monoclonal and polyclonal antibodies, we identified peaks using the findPeaks command in the combined tag directory and annotated with each tag directory using the –log option. A Pearson correlation test was applied to identify correlation between the tag counts. High-confidence peaks were identified using the getDifferentialPeaksReplicates.pl command using the ChIP-seq data obtained with the two antibodies as replicates. Motifs of 8, 10, or 12 nt were identified using the findMotifsGenome.pl command with the parameter –cpg in a window of 100 bp (-size 100). Longer motifs were identified by searching for motifs of lengths more than 15 nt, and the top motif was identified using a length of 30 (-len 30). Optimization of the long motif in the super-binding sites was performed with the parameter –opt.

Statistical analysis

Data (excluding genetic linkage analysis, transcriptome study, and motif analysis) were analyzed with the GraphPad InStat software program, version 6, by using nonparametric Mann-Whitney tests. Differences were considered significant at $P < 0.05$. Detailed protocols for genetic linkage analysis, WES, NGS, Sanger sequencing, comparative genomic hybridization (CGH) array, and transcriptome study can be found in Supplementary Materials and Methods (section S6).

SUPPLEMENTARY MATERIALS

immunology.sciencemag.org/cgi/content/full/3/24/eaat4941/DC1
Section S1. Case reports for families A to D
Section S2. Defective B cell development and T_H17 cell differentiation in HIES patients with *ZNF341* nonsense mutations
Section S3. Exclusion of mutations in *STAT3* in the etiology of the HIES phenotype in family A
Section S4. Identification of *ZNF341* as an AR-HIES–associated gene in a linkage region on chromosome 20 by WES
Section S5. Expression of various *ZNF341* mRNA variants in multiple cell lines and PBMCs
Section S6. Supplementary Materials and Methods
Fig. S1. B and T cell subsets in patient-derived and HD PBMCs.
Fig. S2. Ubiquitous expression of *ZNF341* mRNA in various cell types.
Fig. S3. No association of the genomic region 20q11.22 spanning the *ZNF341* locus with atopy.
Fig. S4. Ectopic expression of ZNF341 variants in HEK293T cells.
Fig. S5. Ectopically expressed wt ZNF341 binds to the *STAT3* promoter leading to transcriptional activation.
Fig. S6. Occupancy by ZNF341 across the *STAT3* promoter as determined by ChIP.
Fig. S7. ZNF341 R386* shows reduced binding to the *STAT3* promoter.
Fig. S8. Flow cytometry gating strategy for in vitro T_H17 cell differentiation assay.
Fig. S9. Flow cytometry gating strategy for Y705 phosphorylation of STAT3.
Fig. S10. Flow cytometry gating strategy for immune phenotyping of PBMCs.
Fig. S11. Flow cytometry gating strategy for IL-22^+ T cells.
Table S1. Clinical and immunological phenotype of HIES patients with *ZNF341* mutations.
Table S2. *ZNF341* encodes three protein coding isoforms.
Table S3. Transcriptome analysis of patient A.II.1 with gene-specific fold changes in comparison to healthy sibling A.II.5.
Table S4. Raw data.
References (*47*–*53*)

REFERENCES AND NOTES

1. E. J. Hillmer, H. Zhang, H. S. Li, S. S. Watowich, STAT3 signaling in immunity. *Cytokine Growth Factor Rev.* **31**, 1–15 (2016).
2. S. Al Khatib, S. Keles, M. Garcia-Lloret, E. Karakoc-Aydiner, I. Reisli, H. Artac, Y. Camcioglu, H. Cokugras, A. Somer, N. Kutukculer, M. Yilmaz, A. Ikinciogullari, O. Yegin, M. Yüksek, F. Genel, E. Kucukosmanoglu, A. Baki, N. N. Bahceciler, A. Rambhatla, D. W. Nickerson, S. McGhee, I. B. Barlan, T. Chatila, Defects along the T_H17 differentiation pathway underlie genetically distinct forms of the hyper IgE syndrome. *J. Allergy Clin. Immunol.* **124**, 342–348.e5 (2009).
3. L. de Beaucoudrey, A. Puel, O. Filipe-Santos, A. Cobat, P. Ghandil, M. Chrabieh, J. Feinberg, H. von Bernuth, A. Samarina, L. Jannière, C. Fieschi, J.-L. Stéphan, C. Boileau, S. Lyonnet, G. Jondeau, V. Cormier-Daire, M. Le Merrer, C. Hoarau, Y. Lebranchu, O. Lortholary, M.-O. Chandesris, F. Tron, E. Gambineri, L. Bianchi, C. Rodriguez-Gallego, S. E. Zitnik, J. Vasconcelos, M. Guedes, A. B. Vitor, L. Marodi, H. Chapel, B. Reid, C. Roifman, D. Nadal, J. Reichenbach, I. Caragol, B.-Z. Garty, F. Dogu, Y. Camcioglu, S. Gülle, O. Sanal, A. Fischer, L. Abel, B. Stockinger, C. Picard, J.-L. Casanova, Mutations in *STAT3* and *IL12RB1* impair the development of human IL-17–producing T cells. *J. Exp. Med.* **205**, 1543–1550 (2008).
4. C. S. Ma, G. Y. J. Chew, N. Simpson, A. Priyadarshi, M. Wong, B. Grimbacher, D. A. Fulcher, S. G. Tangye, M. C. Cook, Deficiency of Th17 cells in hyper IgE syndrome due to mutations in *STAT3*. *J. Exp. Med.* **205**, 1551–1557 (2008).
5. J. D. Milner, J. M. Brenchley, A. Laurence, A. F. Freeman, B. J. Hill, K. M. Elias, Y. Kanno, C. Spalding, H. Z. Elloumi, M. L. Paulson, J. Davis, A. Hsu, A. I. Asher, J. O'Shea,

Downloaded from http://immunology.sciencemag.org/ by guest on September 27, 2020

S. M. Holland, W. E. Paul, D. C. Douek, Impaired T_H17 cell differentiation in subjects with autosomal dominant hyper-IgE syndrome. *Nature* **452**, 773–776 (2008).
6. E. D. Renner, S. Rylaarsdam, S. Añover-Sombke, A. L. Rack, J. Reichenbach, J. C. Carey, Q. Zhu, A. F. Jansson, J. Barboza, L. F. Schimke, M. F. Leppert, M. M. Getz, R. A. Seger, H. R. Hill, B. H. Belohradsky, T. R. Torgerson, H. D. Ochs, Novel signal transducer and activator of transcription 3 (STAT3) mutations, reduced T(H)17 cell numbers, and variably defective STAT3 phosphorylation in hyper-IgE syndrome. *J. Allergy Clin. Immunol.* **122**, 181–187 (2008).
7. P. F. K. Yong, A. F. Freeman, K. R. Engelhardt, S. Holland, J. M. Puck, B. Grimbacher, An update on the hyper-IgE syndromes. *Arthritis Res. Ther.* **14**, 228 (2012).
8. S. E. Flanagan, E. Haapaniemi, M. A. Russell, R. Caswell, H. L. Allen, E. De Franco, T. J. McDonald, H. Rajala, A. Ramelius, J. Barton, K. Heiskanen, T. Heiskanen-Kosma, M. Kajosaari, N. P. Murphy, T. Milenkovic, M. Seppänen, Å. Lernmark, S. Mustjoki, T. Otonkoski, J. Kere, N. G. Morgan, S. Ellard, A. T. Hattersley, Activating germline mutations in *STAT3* cause early-onset multi-organ autoimmune disease. *Nat. Genet.* **46**, 812–814 (2014).
9. J. D. Milner, T. P. Vogel, L. Forbes, C. A. Ma, A. Stray-Pedersen, J. E. Niemela, J. J. Lyons, K. R. Engelhardt, Y. Zhang, N. Topcagic, E. D. O. Roberson, H. Matthews, J. W. Verbsky, T. Dasu, A. Vargas-Hernandez, N. Varghese, K. L. McClain, L. B. Karam, K. Nahmod, G. Makedonas, E. M. Mace, H. S. Sorte, G. Perminow, V. Koneti Rao, M. P. O'Connell, S. Price, H. C. Su, M. Butrick, J. McElwee, J. D. Hughes, J. Willet, D. Swan, Y. Xu, M. Santibanez-Koref, V. Slowik, D. L. Dinwiddie, C. E. Ciaccio, C. J. Saunders, S. Septer, S. F. Kingsmore, A. J. White, A. J. Cant, S. Hambleton, M. A. Cooper, Early-onset lymphoproliferation and autoimmunity caused by germline *STAT3* gain-of-function mutations. *Blood* **125**, 591–599 (2015).
10. S. M. Holland, F. R. DeLeo, H. Z. Elloumi, A. P. Hsu, G. Uzel, N. Brodsky, A. F. Freeman, A. Demidowich, J. Davis, M. L. Turner, V. L. Anderson, D. N. Darnell, P. A. Welch, D. B. Kuhns, D. M. Frucht, H. L. Malech, J. I. Gallin, S. D. Kobayashi, A. R. Whitney, J. M. Voyich, J. M. Musser, C. Woellner, A. A. Schäffer, J. M. Puck, B. Grimbacher, *STAT3* mutations in the hyper-IgE syndrome. *N. Engl. J. Med.* **357**, 1608–1619 (2007).
11. B. Grimbacher, S. M. Holland, J. I. Gallin, F. Greenberg, S. C. Hill, H. L. Malech, J. A. Miller, A. C. O'Connell, J. M. Puck, Hyper-IgE syndrome with recurrent infections—An autosomal dominant multisystem disorder. *N. Engl. J. Med.* **340**, 692–702 (1999).
12. Y. Minegishi, M. Saito, S. Tsuchiya, I. Tsuge, H. Takada, T. Hara, N. Kawamura, T. Ariga, S. Pasic, O. Stojkovic, A. Metin, H. Karasuyama, Dominant-negative mutations in the DNA-binding domain of STAT3 cause hyper-IgE syndrome. *Nature* **448**, 1058–1062 (2007).
13. K. R. Engelhardt, S. McGhee, S. Winkler, A. Sassi, C. Woellner, G. Lopez-Herrera, A. Chen, H. S. Kim, M. G. Lloret, I. Schulze, S. Ehl, J. Thiel, D. Pfeifer, H. Veelken, T. Niehues, K. Siepermann, S. Weinspach, I. Reisli, S. Keles, F. Genel, N. Kütükçüler, Y. Camcioğlu, A. Somer, E. Karakoc-Aydiner, I. Barlan, A. Gennery, A. Metin, A. Degerliyurt, M. C. Pietrogrande, M. Yeganeh, Z. Baz, S. Al-Tamemi, C. Klein, J. M. Puck, S. M. Holland, E. R. B. McCabe, B. Grimbacher, T. A. Chatila, Large deletions and point mutations involving the dedicator of cytokinesis 8 (DOCK8) in the autosomal-recessive form of hyper-IgE syndrome. *J. Allergy Clin. Immunol.* **124**, 1289–302.e4 (2009).
14. Q. Zhang, J. C. Davis, I. T. Lamborn, A. F. Freeman, H. Jing, A. J. Favreau, H. F. Matthews, J. Davis, M. L. Turner, G. Uzel, S. M. Holland, H. C. Su, Combined immunodeficiency associated with DOCK8 mutations. *N. Engl. J. Med.* **361**, 2046–2055 (2009).
15. A. Sassi, S. Lazaroski, G. Wu, S. M. Haslam, M. Fliegauf, F. Mellouli, T. Patiroglu, E. Unal, M. A. Ozdemir, Z. Jouhadi, K. Khadir, L. Ben-Khemis, M. Ben-Ali, I. Ben-Mustapha, L. Borchani, D. Pfeifer, T. Jakob, M. Khemiri, A. C. Asplund, M. O. Gustafsson, K. E. Lundin, E. Falk-Sörqvist, L. N. Moens, H. E. Gungor, K. R. Engelhardt, M. Dziadzio, H. Stauss, B. Fleckenstein, R. Meier, K. Prayitno, A. Maul-Pavicic, S. Schaffer, M. Rakhmanov, P. Henneke, H. Kraus, H. Eibel, U. Kölsch, S. Nadifi, M. Nilsson, M. Bejaoui, A. A. Schäffer, C. I. Smith, A. Dell, M. R. Barbouche, B. Grimbacher, Hypomorphic homozygous mutations in *Phosphoglucomutase 3* (PGM3) impair immunity and increase serum IgE levels. *J. Allergy Clin. Immunol.* **133**, 1410–1419.e13 (2014).
16. Y. Zhang, X. Yu, M. Ichikawa, J. J. Lyons, S. Datta, I. T. Lamborn, H. Jing, E. S. Kim, M. Biancalana, L. A. Wolfe, T. DiMaggio, H. F. Matthews, S. M. Kranick, K. D. Stone, S. M. Holland, D. S. Reich, J. D. Hughes, H. Mehmet, J. McElwee, A. F. Freeman, H. H. Freeze, H. C. Su, J. D. Milner, Autosomal recessive phosphoglucomutase 3 (*PGM3*) mutations link glycosylation defects to atopy, immune deficiency, autoimmunity, and neurocognitive impairment. *J. Allergy Clin. Immunol.* **133**, 1400–1409.e5 (2014).
17. S. Keles, L. M. Charbonnier, V. Kabaleeswaran, I. Reisli, F. Genel, N. Gulez, W. Al-Herz, N. Ramesh, A. Perez-Atayde, N. E. Karaca, N. Kutukculer, H. Wu, R. S. Geha, T. A. Chatila, Dedicator of cytokinesis 8 regulates signal transducer and activator of transcription 3 activation and promotes T_H17 cell differentiation. *J. Allergy Clin. Immunol.* **138**, 1384–1394.e2 (2016).
18. C. S. Ma, D. T. Avery, A. Chan, M. Batten, J. Bustamante, S. Boisson-Dupuis, P. D. Arkwright, A. Y. Kreins, D. Averbuch, D. Engelhard, K. Magdorf, S. S. Kilic, Y. Minegishi, S. Nonoyama, M. A. French, S. Choo, J. M. Smart, J. Peake, M. Wong, P. Gray, M. C. Cook, D. A. Fulcher, J.-L. Casanova, E. K. Deenick, S. G. Tangye, Functional STAT3 deficiency compromises the generation of human T follicular helper cells. *Blood* **119**, 3997–4008 (2012).
19. K. Shuai, B. Liu, Regulation of JAK–STAT signalling in the immune system. *Nat. Rev. Immunol.* **3**, 900–911 (2003).
20. Y. J. Xu, L. Li, Y. Chen, B. Fu, D. S. Wu, X. L. Li, X. L. Zhao, F. P. Chen, Role of HMGB1 in regulation of STAT3 expression in $CD4^+$ T cells from patients with aGVHD after allogeneic hematopoietic stem cell transplantation. *Clin. Immunol.* **161**, 278–283 (2015).
21. Y. Cheng, H. Geng, S. H. Cheng, P. Liang, Y. Bai, J. Li, G. Srivastava, M. H. L. Ng, T. Fukagawa, X. Wu, A. T. C. Chan, Q. Tao, KRAB zinc finger protein ZNF382 is a proapoptotic tumor suppressor that represses multiple oncogenes and is commonly silenced in multiple carcinomas. *Cancer Res.* **70**, 6516–6526 (2010).
22. L. Lin, Z. Yao, K. Bhuvaneshwar, Y. Gusev, B. Kallakury, S. Yang, K. Shetty, A. R. He, Transcriptional regulation of *STAT3* by SPTBN1 and SMAD3 in HCC through cAMP-response element-binding proteins ATF3 and CREB2. *Carcinogenesis* **35**, 2393–2403 (2014).
23. M. A. Kluger, S. Melderis, A. Nosko, B. Goerke, M. Luig, M. C. Meyer, J. E. Turner, C. Meyer-Schwesinger, C. Wegscheid, G. Tiegs, R. A. Stahl, U. Panzer, O. M. Steinmetz, Treg17 cells are programmed by Stat3 to suppress Th17 responses in systemic lupus. *Kidney Int.* **89**, 158–166 (2016).
24. L. Paternoster, M. Standl, J. Waage, H. Baurecht, M. Hotze, D. P. Strachan, J. A. Curtin, K. Bønnelykke, C. Tian, A. Takahashi, J. Esparza-Gordillo, A. C. Alves, J. P. Thyssen, H. T. den Dekker, M. A. Ferreira, E. Altmaier, P. M. Sleiman, F. L. Xiao, J. R. Gonzalez, I. Marenholz, B. Kalb, M. P. Yanes, C. J. Xu, L. Carstensen, M. M. Groen-Blokhuis, C. Venturini, C. E. Pennell, S. J. Barton, A. M. Levin, I. Curjuric, M. Bustamante, E. Kreiner-Møller, G. A. Lockett, J. Bacelis, S. Bunyavanich, R. A. Myers, A. Matanovic, A. Kumar, J. Y. Tung, T. Hirota, M. Kubo, W. L. McArdle, A. J. Henderson, J. P. Kemp, J. Zheng, G. D. Smith, F. Rüschendorf, A. Bauerfeind, M. A. Lee-Kirsch, A. Arnold, G. Homuth, C. O. Schmidt, E. Mangold, S. Cichon, T. Keil, E. Rodríguez, A. Peters, A. Franke, W. Lieb, N. Novak, R. Fölster-Holst, M. Horikoshi, J. Pekkanen, S. Sebert, L. L. Husemoen, N. Grarup, J. C. de Jongste, F. Rivadeneira, A. Hofman, V. W. Jaddoe, S. G. Pasmans, N. J. Elbert, A. G. Uitterlinden, G. B. Marks, P. J. Thompson, M. C. Matheson, C. F. Robertson; Australian Asthma Genetics Consortium (AAGC), J. S. Ried, J. Li, X. B. Zuo, X. D. Zheng, X. Y. Yin, L. D. Sun, M. A. McAleer, G. M. O'Regan, C. M. Fahy, L. E. Campbell, M. Macek, M. Kurek, D. Hu, C. Eng, D. S. Postma, B. Feenstra, F. Geller, J. J. Hottenga, C. M. Middeldorp, P. Hysi, V. Bataille, T. Spector, C. M. Tiesler, E. Thiering, B. Pahukasahasram, J. J. Yang, M. Imboden, S. Huntsman, N. Vilor-Tejedor, C. L. Relton, R. Myhre, W. Nystad, A. Custovic, S. T. Weiss, D. A. Meyers, C. Söderhäll, E. Melén, C. Ober, B. A. Raby, A. Simpson, B. Jacobsson, J. W. Holloway, H. Bisgaard, J. Sunyer, N. M. P. Hensch, L. K. Williams, K. M. Godfrey, C. A. Wang, D. I. Boomsma, M. Melbye, G. H. Koppelman, D. Jarvis, W. I. McLean, A. D. Irvine, X. J. Zhang, H. Hakonarson, C. Gieger, E. G. Burchard, N. G. Martin, L. Duijts, A. Linneberg, M. R. Jarvelin, M. M. Noethen, S. Lau, N. Hübner, Y. A. Lee, M. Tamari, D. A. Hinds, D. Glass, S. J. Brown, J. Heinrich, D. M. Evans, S. Weidinger, Multi-ancestry genome-wide association study of 21,000 cases and 95,000 controls identifies new risk loci for atopic dermatitis. *Nat. Genet.* **47**, 1449–1456 (2015).
25. K. Bønnelykke, M. C. Matheson, T. H. Pers, R. Granell, D. P. Strachan, A. C. Alves, A. Linneberg, J. A. Curtin, N. M. Warrington, M. Standl, M. Kerkhof, I. Jonsdottir, B. K. Bukvic, M. Kaakinen, P. Sleiman, G. Thorleifsson, U. Thorsteinsdottir, K. Schramm, S. Baltic, E. Kreiner-Møller, A. Simpson, B. St Pourcain, L. Coin, J. Hui, E. H. Walters, C. M. T. Tiesler, D. L. Duffy, G. Jones; AAGC, S. M. Ring, W. L. McArdle, L. Price, C. F. Robertson, J. Pekkanen, C. S. Tang, E. Thiering, G. W. Montgomery, A. L. Hartikainen, S. C. Dharmage, L. L. Husemoen, C. Herder, J. P. Kemp, P. Elliot, A. James, M. Waldenberger, M. J. Abramson, B. P. Fairfax, J. C. Knight, R. Gupta, P. J. Thompson, P. Holt, P. Sly, J. N. Hirschhorn, M. Blekic, S. Weidinger, H. Hakonarsson, K. Stefansson, J. Heinrich, D. S. Postma, A. Custovic, C. E. Pennell, M. R. Jarvelin, G. H. Koppelman, N. Timpson, M. A. Ferreira, H. Bisgaard, A. J. Henderson, Meta-analysis of genome-wide association studies identifies ten loci influencing allergic sensitization. *Nat. Genet.* **45**, 902–906 (2013).
26. D. Welter, J. MacArthur, J. Morales, T. Burdett, P. Hall, H. Junkins, A. Klemm, P. Flicek, T. Manolio, L. Hindorff, H. Parkinson, The NHGRI GWAS Catalog, a curated resource of SNP-trait associations. *Nucleic Acids Res.* **42**, D1001–D1006 (2014).
27. W. J. Leonard, J. J. O'Shea, Jaks and STATs: Biological implications. *Annu. Rev. Immunol.* **16**, 293–322 (1998).
28. D. E. Levy, J. E. Darnell Jr., Stats: Transcriptional control and biological impact. *Nat. Rev. Mol. Cell Biol.* **3**, 651–662 (2002).
29. A. V. Villarino, Y. Kanno, J. J. O'Shea, Mechanisms and consequences of Jak-STAT signaling in the immune system. *Nat. Immunol.* **18**, 374–384 (2017).
30. J.-L. Casanova, S. M. Holland, L. D. Notarangelo, Inborn errors of human JAKs and STATs. *Immunity* **36**, 515–528 (2012).
31. K. Ghoreschi, A. Laurence, J. J. O'Shea, Janus kinases in immune cell signaling. *Immunol. Rev.* **228**, 273–287 (2009).
32. W. Vainchenker, A. Dusa, S. N. Constantinescu, JAKs in pathology: Role of Janus kinases in hematopoietic malignancies and immunodeficiencies. *Semin. Cell Dev. Biol.* **19**, 385–393 (2008).

Downloaded from http://immunology.sciencemag.org/ by guest on September 27, 2020

33. L. Liu, S. Okada, X.-F. Kong, A. Y. Kreins, S. Cypowyj, A. Abhyankar, J. Toubiana, Y. Itan, M. Audry, P. Nitschke, C. Masson, B. Toth, J. Flatot, M. Migaud, M. Chrabieh, T. Kochetkov, A. Bolze, A. Borghesi, A. Toulon, J. Hiller, S. Eyerich, K. Eyerich, V. Gulácsy, L. Chernyshova, V. Chernyshov, A. Bondarenko, R. M. C. Grimaldo, L. Blancas-Galicia, I. M. M. Beas, J. Roesler, K. Magdorf, D. Engelhard, C. Thumerelle, P.-R. Burgel, M. Hoernes, B. Drexel, R. Seger, T. Kusuma, A. F. Jansson, J. Sawalle-Belohradsky, B. Belohradsky, E. Jouanguy, J. Bustamante, M. Bué, N. Karin, G. Wildbaum, C. Bodemer, O. Lortholary, A. Fischer, S. Blanche, S. Al-Muhsen, J. Reichenbach, M. Kobayashi, F. E. Rosales, C. T. Lozano, S. S. Kilic, M. Oleastro, A. Etzioni, C. Traidl-Hoffmann, E. D. Renner, L. Abel, C. Picard, L. Maródi, S. Boisson-Dupuis, A. Puel, J.-L. Casanova, Gain-of-function human *STAT1* mutations impair IL-17 immunity and underlie chronic mucocutaneous candidiasis. *J. Exp. Med.* **208**, 1635–1648 (2011).
34. D. Averbuch, A. Chapgier, S. Boisson-Dupuis, J.-L. Casanova, D. Engelhard, The clinical spectrum of patients with deficiency of signal transducer and activator of transcription-1. *Pediatr. Infect. Dis. J.* **30**, 352–355 (2011).
35. S. Boisson-Dupuis, X.-F. Kong, S. Okada, S. Cypowyj, A. Puel, L. Abel, J.-L. Casanova, Inborn errors of human STAT1: Allelic heterogeneity governs the diversity of immunological and infectious phenotypes. *Curr. Opin. Immunol.* **24**, 364–378 (2012).
36. S. Baris, F. Alroqi, A. Kiykim, E. Karakoc-Aydiner, I. Ogulur, A. Ozen, L.-M. Charbonnier, M. Bakır, K. Boztug, T. A. Chatila, I. B. Barlan, Severe early-onset combined immunodeficiency due to heterozygous gain-of-function mutations in *STAT1*. *J. Clin. Immunol.* **36**, 641–648 (2016).
37. F. Dhalla, H. Fox, E. E. Davenport, R. Sadler, C. Anzilotti, P. A. van Schouwenburg, B. Ferry, H. Chapel, J. C. Knight, S. Y. Patel, Chronic mucocutaneous candidiasis: Characterization of a family with STAT-1 gain-of-function and development of an ex-vivo assay for Th17 deficiency of diagnostic utility. *Clin. Exp. Immunol.* **184**, 216–227 (2016).
38. J. Toubiana, S. Okada, J. Hiller, M. Oleastro, M. L. Gomez, J. C. A. Becerra, M. Ouachée-Chardin, F. Fouyssac, K. Mohan Girisha, A. Etzioni, J. Van Montfrans, Y. Camcioglu, L. Ann Kerns, B. Belohradsky, S. Blanche, A. Bousfiha, C. Rodriguez-Gallego, I. Meyts, K. Kisand, J. Reichenbach, E. D. Renner, S. Rosenzweig, B. Grimbacher, F. L. van de Veerdonk, C. Traidl-Hoffmann, C. Picard, L. Marodi, T. Morio, M. Kobayashi, D. Lilic, J. D. Milner, S. Holland, J.-L. Casanova, A. Puel; International STAT1 Gain-of-Function Study Group, Heterozygous *STAT1* gain-of-function mutations underlie an unexpectedly broad clinical phenotype. *Blood* **127**, 3154–3164 (2016).
39. H. L. Koskela, S. Eldfors, P. Ellonen, A. J. van Adrichem, H. Kuusanmäki, E. I. Andersson, S. Lagström, M. J. Clemente, T. Olson, S. E. Jalkanen, M. M. Majumder, H. Almusa, H. Edgren, M. Lepistö, P. Mattila, K. Guinta, P. Koistinen, T. Kuittinen, K. Penttinen, A. Parsons, J. Knowles, J. Saarela, K. Wennerberg, O. Kallioniemi, K. Porkka, T. P. Loughran Jr., C. A. Heckman, J. P. Maciejewski, S. Mustjoki, Somatic STAT3 mutations in large granular lymphocytic leukemia. *N. Engl. J. Med.* **366**, 1905–1913 (2012).
40. D. M. Schwartz, M. Bonelli, M. Gadina, J. J. O'Shea, Type I/II cytokines, JAKs, and new strategies for treating autoimmune diseases. *Nat. Rev. Rheumatol.* **12**, 25–36 (2016).
41. E. Higgins, T. Al Shehri, M. A. McAleer, N. Conlon, C. Feighery, D. Lilic, A. D. Irvine, Use of ruxolitinib to successfully treat chronic mucocutaneous candidiasis caused by gain-of-function signal transducer and activator of transcription 1 (STAT1) mutation. *J. Allergy Clin. Immunol.* **135**, 551–553 (2015).
42. R. Mössner, N. Diering, O. Bader, S. Forkel, T. Overbeck, U. Gross, B. Grimbacher, M. P. Schön, T. Buhl, Ruxolitinib induces interleukin 17 and ameliorates chronic mucocutaneous candidiasis caused by STAT1 gain-of-function mutation. *Clin. Infect. Dis.* **62**, 951–953 (2016).
43. A. Klug, The discovery of zinc fingers and their applications in gene regulation and genome manipulation. *Annu. Rev. Biochem.* **79**, 213–231 (2010).
44. F. Millan, M. T. Cho, K. Retterer, K. G. Monaghan, R. Bai, P. Vitazka, D. B. Everman, B. Smith, B. Angle, V. Roberts, L. Immken, H. Nagakura, M. DiFazio, E. Sherr, E. Haverfield, B. Friedman, A. Telegrafi, J. Juusola, W. K. Chung, S. Bale, Whole exome sequencing reveals de novo pathogenic variants in *KAT6A* as a cause of a neurodevelopmental disorder. *Am. J. Med. Genet. A* **170**, 1791–1798 (2016).
45. F. W. Schmitges, E. Radovani, H. S. Najafabadi, M. Barazandeh, L. F. Campitelli, Y. Yin, A. Jolma, G. Zhong, H. Guo, T. Kanagalingam, W. F. Dai, J. Taipale, A. Emili, J. F. Greenblatt, T. R. Hughes, Multiparameter functional diversity of human C2H2 zinc finger proteins. *Genome Res.* **26**, 1742–1752 (2016).
46. K. Kato, M. Nomoto, H. Izumi, T. Ise, S. Nakano, Y. Niho, K. Kohno, Structure and functional analysis of the human STAT3 gene promoter: Alteration of chromatin structure as a possible mechanism for the upregulation in cisplatin-resistant cells. *Biochim. Biophys. Acta* **1493**, 91–100 (2000).
47. B. Grimbacher, A. A. Schäffer, S. M. Holland, J. Davis, J. I. Gallin, H. L. Malech, T. P. Atkinson, B. H. Belohradsky, R. H. Buckley, F. Cossu, T. Español, B. Z. Garty, N. Matamoros, L. A. Myers, R. P. Nelson, H. D. Ochs, E. D. Renner, N. Wellinghausen, J. M. Puck, Genetic linkage of hyper-IgE syndrome to chromosome 4. *Am. J. Hum. Genet.* **65**, 735–744 (1999).
48. C. Speckmann, A. Enders, C. Woellner, D. Thiel, A. Rensing-Ehl, M. Schlesier, J. Rohr, T. Jakob, E. Oswald, M. V. Kopp, O. Sanal, J. Litzman, A. Plebani, M. C. Pietrogrande, J. L. Franco, T. Espanol, B. Grimbacher, S. Ehl, Reduced memory B cells in patients with hyper IgE syndrome. *Clin. Immunol.* **129**, 448–454 (2008).
49. A. Finck, J. W. Van der Meer, A. A. Schäffer, J. Pfannstiel, C. Fieschi, A. Plebani, A. D. Webster, L. Hammarström, B. Grimbacher, Linkage of autosomal-dominant common variable immunodeficiency to chromosome 4q. *Eur. J. Hum. Genet.* **14**, 867–875 (2006).
50. G. Lopez-Herrera, G. Tampella, Q. Pan-Hammarström, P. Herholz, C. M. Trujillo-Vargas, K. Phadwal, A. K. Simon, M. Moutschen, A. Etzioni, A. Mory, I. Srugo, D. Melamed, K. Hultenby, C. Liu, M. Baronio, M. Vitali, P. Philippet, V. Dideberg, A. Aghamohammadi, N. Rezaei, V. Enright, L. Du, U. Salzer, H. Eibel, D. Pfeifer, H. Veelken, H. Stauss, V. Lougaris, A. Plebani, E. M. Gertz, A. A. Schäffer, L. Hammarström, B. Grimbacher, Deleterious mutations in *LRBA* are associated with a syndrome of immune deficiency and autoimmunity. *Am. J. Hum. Genet.* **90**, 986–1001 (2012).
51. R. W. Cottingham Jr., R. M. Idury, A. A. Schaffer, Faster sequential genetic linkage computations. *Am. J. Hum. Genet.* **53**, 252–263 (1993).
52. G. M. Lathrop, J. M. Lalouel, C. Julier, J. Ott, Strategies for multilocus linkage analysis in humans. *Proc. Natl. Acad. Sci. U.S.A.* **81**, 3443–3446 (1984).
53. A. A. Schaffer, S. K. Gupta, K. Shriram, R. W. Cottingham Jr., Avoiding recomputation in linkage analysis. *Hum. Hered.* **44**, 225–237 (1994).

Acknowledgments: We are grateful to all affected individuals, their families, and all HD controls who participated in this study. We thank D. Thiel, P. Mrovecova, K. Hübscher, M. Buchta, H. Haberstroh, N. Glaser, and T. Stauss for their excellent technical assistance. We thank M. Schmidt and I. Müller-Fleckenstein for generating patients' T cell lines at the Institute of Clinical and Molecular Virology, University of Erlangen-Nürnberg. We thank G. Finkenzeller for providing PSFs of an HD from the Plastic Surgery, Medical Center, University of Freiburg. We thank M. Leipold for performing the CGH array (section S3) at the Institute of Human Genetics, University of Freiburg. Sequencing for ChIP-seq was conducted at the Genomics Core Facility of the European Molecular Biology Laboratories. We thank the microarray unit of the Deutsches Krebsforschungszentrum Genomics and Proteomics Core Facility for providing the Illumina Whole-Genome Expression Beadchips (transcriptome study) and related services. **Funding:** Financial support for this research came from the German Ministry of Education and Research (grant number 01E01303 and sysINFLAME grant numbers 01ZX1306F and 01ZX1306A), the Intramural Research Program of the NIH, National Library of Medicine, the E-rare program of the European Commission EURO-CMC (01GM1502, ANR-14-RARE-0005-02), the NIH (R01AI127564), the Jeffrey Modell Foundation Translational Research Program, the German Center for Infection Research, and the Deutsche Forschungsgemeinschaft (SFB1160-IMPATH). The funding organizations had no role in study design; the collection, analysis, and interpretation of data; the writing of the report; or the decision to submit the paper for publication. The authors are responsible for the content of this research. J.M.H. is a fellow of the MOTI-VATE graduate program of the Medical Faculty of Freiburg. **Author contributions:** B.G., A.E., B.-Z.G., and S.S.K. initiated the project; A.K., I.L., I.L.-R., S.S.K., B.-Z.G., and A.E. took care of the patients; S.F.-J., J.M.H., M.F., C.B., M.L.W., J.C.N., M.P., P.F., C.N., L.Y., J.R.-R., N.L., S. Winzer, C.G., B.F., and B.G. designed and/or performed experiments and analyzed results; A.B., S. Winzer, K.R.E., C.G., D.P., S. Weidinger, and A.A.S. performed genetic analysis; V.B., A.P., and J.-L.C. created and provided reagents; S.F.-J., J.M.H., M.F., C.B., C.N., J.C.N., and M.P. prepared the figures; S.F.-J., J.M.H., M.F., C.B., M.L.W., J.C.N., C.N., and L.Y. performed statistical analysis; and S.F.-J., J.M.H., M.F., C.B., and B.G. drafted the paper. **Competing interests:** The authors declare that they have no competing interests. **Data and materials availability:** Data accession number: ChIP-seq, GSE107719; transcriptome study, GSE109030.

Submitted 5 March 2018
Accepted 17 May 2018
Published 15 June 2018
10.1126/sciimmunol.aat4941

Citation: S. Frey-Jakobs, J. M. Hartberger, M. Fliegauf, C. Bossen, M. L. Wehmeyer, J. C. Neubauer, A. Bulashevska, M. Proietti, P. Fröbel, C. Nöltner, L. Yang, J. Rojas-Restrepo, N. Langer, S. Winzer, K. R. Engelhardt, C. Glocker, D. Pfeifer, A. Klein, A. A. Schäffer, I. Lagovsky, I. Lachover-Roth, V. Béziat, A. Puel, J.-L. Casanova, B. Fleckenstein, S. Weidinger, S. S. Kilic, B.-Z. Garty, A. Etzioni, B. Grimbacher, ZNF341 controls STAT3 expression and thereby immunocompetence. *Sci. Immunol.* **3**, eaat4941 (2018).

Downloaded from http://immunology.sciencemag.org/ by guest on September 27, 2020

Science Immunology

ZNF341 controls STAT3 expression and thereby immunocompetence

Stefanie Frey-Jakobs, Julia M. Hartberger, Manfred Fliegauf, Claudia Bossen, Magdalena L. Wehmeyer, Johanna C. Neubauer, Alla Bulashevska, Michele Proietti, Philipp Fröbel, Christina Nöltner, Linlin Yang, Jessica Rojas-Restrepo, Niko Langer, Sandra Winzer, Karin R. Engelhardt, Cristina Glocker, Dietmar Pfeifer, Adi Klein, Alejandro A. Schäffer, Irina Lagovsky, Idit Lachover-Roth, Vivien Béziat, Anne Puel, Jean-Laurent Casanova, Bernhard Fleckenstein, Stephan Weidinger, Sara S. Kilic, Ben-Zion Garty, Amos Etzioni and Bodo Grimbacher

Sci. Immunol. **3**, eaat4941.
DOI: 10.1126/sciimmunol.aat4941

Fingers on the trigger

Hyper–immunoglobulin E syndromes (HIESs) are rare genetic immunodeficiency diseases characterized by bacterial infections, chronic mucocutaneous candidiasis, allergies, and skeletal abnormalities that are associated with excessive T_H2 responses and impaired T_H17 immunity. Béziat *et al*. and Frey-Jakobs *et al*. have studied patients with an autosomal recessive form of HIES and identified mutations in the zinc finger transcription factor ZNF341 as the culprit. Loss-of-function mutations encoding truncated forms of ZNF341 interfered with its ability to recognize a bipartite binding site located in the promoter of STAT3, the transcription factor mutated in most cases of autosomal dominant HIES. ZNF341-supported transcription of STAT3 is a key upstream regulatory step needed to trigger the normal induction of the T_H17 differentiation pathway. These findings reveal a previously unappreciated layer of transcriptional regulation controlling JAK-STAT signaling.

ARTICLE TOOLS http://immunology.sciencemag.org/content/3/24/eaat4941

SUPPLEMENTARY MATERIALS http://immunology.sciencemag.org/content/suppl/2018/06/12/3.24.eaat4941.DC1

REFERENCES This article cites 53 articles, 9 of which you can access for free
http://immunology.sciencemag.org/content/3/24/eaat4941#BIBL

Use of this article is subject to the Terms of Service

Science Immunology (ISSN 2470-9468) is published by the American Association for the Advancement of Science, 1200 New York Avenue NW, Washington, DC 20005. The title *Science Immunology* is a registered trademark of AAAS.

Copyright © 2018 The Authors, some rights reserved; exclusive licensee American Association for the Advancement of Science. No claim to original U.S. Government Works

Downloaded from http://immunology.sciencemag.org/ by guest on September 27, 2020